Understanding the Crystal Structure of Layered $LiNi_{0.5}Mn_{0.5}O_2$ by Electron Diffraction and Powder Diffraction Simulation

Y. S. Meng,[a] G. Ceder,[a,b,*] C. P. Grey,[c,*] W.-S. Yoon,[d,*] and Y. Shao-Horn[e,*,z]

[a]*Advanced Materials for Micro- and Nano-Systems, Singapore-MIT Alliance, Singapore 117576*
[b]*Department of Materials Science and Engineering, Massachusetts Institute of Technology, Cambridge, Massachusetts 02139, USA*
[c]*Department of Chemistry, State University of New York at Stony Brook, Stony Brook, New York 11794, USA*
[d]*Brookhaven National Laboratory, Materials Science Division, Upton, New York 11973, USA*
[e]*Department of Mechanical Engineering, Massachusetts Institute of Technology, Cambridge, Massachusetts 02139, USA*

A combination of experimental techniques that probe different relevant length scales is necessary to truly understand the structure of complex solids. In $LiNi_{0.5}Mn_{0.5}O_2$ electron diffraction reveals the presence of long-range ordering, previously undetected with X-ray diffraction and neutron diffraction. We propose a superstructure for this material with space group $P3_112$, and a $\sqrt{3}a_{hex.} \times \sqrt{3}a_{hex.}$ ordering in the transition metal layers. Surprisingly, these ordered layers are stacked in *abcabc* sequence along the *c* axis, indicating the presence of long-range interactions between different transition-metal layers. Electron diffraction evidence indicates that Li, Ni, and Mn ions are not distributed randomly in the transition-metal layers, but order and form two sublattices with significantly different occupation. We further demonstrate that this ordering would be extremely difficult to detect experimentally, if not impossible, with powder diffraction by X-rays and neutrons.
© 2004 The Electrochemical Society. [DOI: 10.1149/1.1718211] All rights reserved.

Layered lithium nickel manganese oxides have been reported as promising positive electrode materials for advanced lithium rechargeable batteries.[1-3] The material $LiNi_{0.5}Mn_{0.5}O_2$ shows stable reversible capacity up to 200 mAh/g in the potential window of 2.5-4.5 V.[4] Although various computational and experimental methods have been undertaken to study this material,[3,5,6] the details of the structure of $LiNi_{0.5}Mn_{0.5}O_2$ are not fully understood and are still subject to debate.

In $LiNi_{0.5}Mn_{0.5}O_2$ the nickel and manganese ions have a valence state of 2+ and 4+, respectively, as suggested by a first-principles study[6] and later confirmed by X-ray absorption near-edge fine structure (XANES) results.[7] Using X-ray powder diffraction (XRD), the structure of $LiNi_{0.5}Mn_{0.5}O_2$ is usually indexed as a rhombohedral layered structure with space group $R\bar{3}m$. The separation of Li and transition metals in different layers is not perfect in $LiNi_{0.5}Mn_{0.5}O_2$, as Rietveld refinement of the structure based on XRD and neutron diffraction data gives 8-10% Ni ions in the Li layer.[1,3,8] Such mixing is naturally accompanied by the presence of Li ions in the transition-metal (Ni, Mn) layers, which has been revealed by ^{6}Li magic-angle spinning (MAS) NMR studies.[5,9]

$LiNi_{0.5}Mn_{0.5}O_2$ represents the end member of the solid solution $Li[Ni_xLi_{1/3-2x/3}Mn_{2/3-x/3}]O_2$ ($0 < x \leq 1/2$). From powder XRD studies, Lu *et al.* proposed that for $0 < x < 1/3$ in $Li[Ni_xLi_{1/3-2x/3}Mn_{2/3-x/3}]O_2$ Ni, Mn and Li ions are ordered in the transition-metal layer on a $\sqrt{3}a_{hex.} \times \sqrt{3}a_{hex.}$ superlattice.[8] They reported that ordering is not expected for the composition $x = 1/2$ as X-ray and neutron powder diffraction analyses reveal little indication of superlattice peaks.[8] However, recent first-principles computation and Li-NMR analyses[10] reveal strong ordering interactions between Ni^{2+} and Mn^{4+}, and Li^+ and Mn^{4+}, even for this composition. Monte Carlo simulations on perfectly stoichiometric material show that short-range ordering of Ni^{2+} and Mn^{4+} is retained near synthesis temperature range, although these simulations do not account for the presence of Li in the transition-metal layer.[10] NMR data reveal a preference for Li in the transition-metal layers to be surrounded by Mn.[10] Moreover, recent electron diffraction data of a $LiNi_{0.5}Mn_{0.5}O_2$ sample by Ohzuku and Makimura clearly reveal a

$\sqrt{3}a_{hex.} \times \sqrt{3}a_{hex.}$ superstructure relative to the parent hexagonal cell, but a detailed structural model was not discussed.[11]

In this article, we combine experimental electron diffraction data of a $LiNi_{0.5}Mn_{0.5}O_2$ sample with diffraction simulations to demonstrate that (Li, Ni, and Mn) are coherently ordered in the transition-metal layers over large enough ranges so as to give superstructure reflections. We also propose a complete description of the unit cell by giving careful consideration to the possible stacking sequences of the ordered transition-metal layers.

A $LiNi_{0.5}Mn_{0.5}O_2$ sample was synthesized from stoichiometric quantities of coprecipitated manganese and nickel hydroxides with ^{6}Li enriched (Isotec) lithium hydroxide at 900°C for 24 h in O_2. NMR results for this sample indicated an occupancy for Li in the Ni/Mn layers of 7 ± 1.5%.[10] XRD data indicated the formation of a layered structure with space group $R\bar{3}m$ with about 9% Ni in the lithium layer. Electron diffraction patterns and transmission electron microscope (TEM) images were collected from the $LiNi_{0.5}Mn_{0.5}O_2$ powder sample, which was suspended on a copper grid with lacey carbon under an accelerating voltage of 200 keV on a JEOL 200CX, JEOL 2000FX, or JEOL 2010 microscope. Chemical analyses of Ni and Mn contents of individual $LiNi_{0.5}Mn_{0.5}O_2$ crystals were performed by X-ray energy dispersive spectroscopy (EDS) at a sample tilt angle of +15° (tilted toward the X-ray detector) on the JEOL
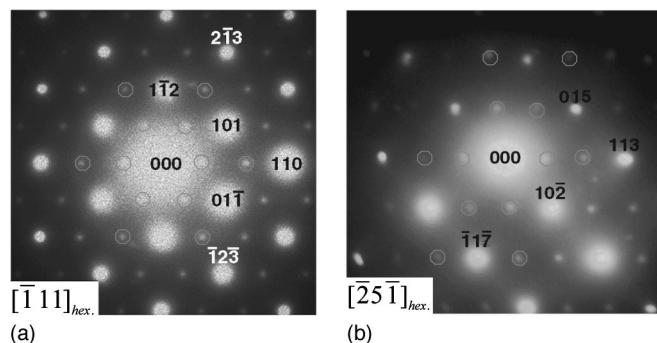
Figure 1. (a) $[\bar{1}11]_{hex.}$ (b) $[\bar{2}5\bar{1}]_{hex.}$ electron diffraction patterns of $LiNi_{0.5}Mn_{0.5}O_2$, fundamental reflections indexed based on parent hexagonal cell. Tripling superreflections of the (11*l*) type planes are circled for clarification.

* Electrochemical Society Active Member.
z E-mail: shaohorn@mit.edu
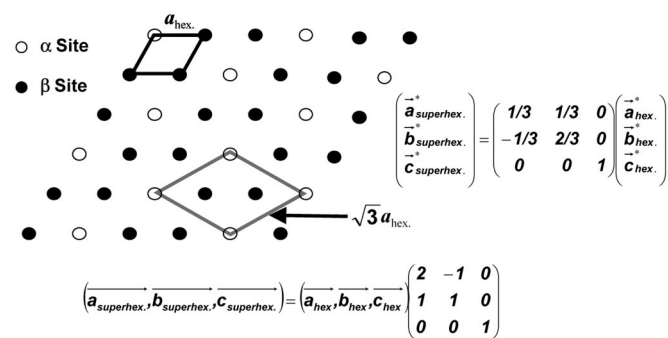
Figure 2. Schematic of in-plane cation ordering in the transition-metal layer in $LiNi_{0.5}Mn_{o.5}O_2$. Multiplicity of α and β are 1/3 and 2/3, respectively, in a triangular lattice plane. The transformation matrix of the $\sqrt{3}a_{\text{hex.}} \times \sqrt{3}a_{\text{hex.}} \times c_{\text{hex.}}$ superstructure with respect to the parent hexagonal cell is presented.

2010 microscope. Examination of ten randomly selected single crystals revealed an average composition of $LiMn_{0.51}Ni_{0.49}O_2$, which agrees with the nominal composition within experimental uncertainty. Lithium and oxygen contents were not quantified by EDS and were assumed stoichiometric.

A total of 34 electron diffraction patterns were collected randomly from the $LiNi_{0.5}Mn_{0.5}O_2$ sample. Among those patterns, 17 revealed superstructure reflections in addition to the fundamental reflections of the hexagonal parent structure with trigonal symmetry $R\bar{3}m$. The most predominant feature of electron diffraction patterns with commensurate superreflections is that only the $(11l)_{\text{hex.}}$ planar spacings ($l = 3n$, $n = 0$, ± 1, $\pm 2...$) in the parent hexagonal structure were tripled by the presence of the superreflections. Figure 1a and b, respectively, shows the $[\bar{1}11]_{\text{hex.}}$ and $[\bar{2}5\bar{1}]_{\text{hex.}}$ zone axis patterns with fundamental reflections indexed to the parent hexagonal cell (space group $R\bar{3}m$) with lattice parameters $a_{\text{hex.}} = 2.895$ Å and $c_{\text{hex.}} = 14.311$ Å.[9,10] The presence of these unique superstructure reflections suggests the formation of a $\sqrt{3}a_{\text{hex.}} \times \sqrt{3}a_{\text{hex.}} \times c_{\text{hex.}}$ superstructure, which implies long-range ordering in the transition-metal layer in the $LiNi_{0.5}Mn_{0.5}O_2$ sample.

Ordering in a $\sqrt{3} \times \sqrt{3}$ superstructure cell (Fig. 2) is common on triangular lattices, and has been observed for Li-vacancy ordering in Li_xCoO_2[12,13] and Li_xNiO_2[14] at $x = 1/3$. This superstructure creates

two distinct sites (α and β) in the transition-metal layer with a multiplicity of 1 and 2. As the translational unit in the transition metal layer is enlarged by the superstructure formation, different ways of positioning successive transition-metal layers along the c axis are possible. The *abcabc* stacking of the ordered transition metal layers in Fig. 3a creates a superstructure with $P3_112$ symmetry, which consists of three transition-metal layers per unit cell. Projection of three successive transition-metal layers along the c axis, as shown in Fig. 3b, illustrates that the structure has a threefold screw axis. The stacking shown in Fig. 3c (*ababab* stacking) leads to $C2/m$ symmetry and is equivalent to the unit cell of Li_2MnO_3. In Li_2MnO_3 pure layers of Li alternate with layers of composition $Li_{1/3}Mn_{2/3}$ in which Li and Mn ions are ordered in the $\sqrt{3}a_{\text{hex.}} \times \sqrt{3}a_{\text{hex.}}$ superstructure of Fig. 2.[15] Projection of two successive transition-metal layers of Li_2MnO_3 shows that the structure has no threefold screw axis but a twofold axis and an in-plane mirror plane $(2/m)$ in Fig. 3d.

Careful comparison of the TEM patterns with electron diffraction simulations of these two possible stackings of the transition metal layers indicates that $LiNi_{0.5}Mn_{0.5}O_2$ has three transition-metal layers per unit cell with space group $P3_112$. For example, tripling of the $(113)_{\text{hex.}}$ type fundamental reflections in Fig. 1b is consistent with the $\sqrt{3}a_{\text{hex.}} \times \sqrt{3}a_{\text{hex.}} \times c_{\text{hex.}}$ superstructure with space group $P3_112$: these superreflections are absent when the electron diffraction pattern of $LiNi_{0.5}Mn_{0.5}O_2$ is simulated along the equivalent zone axis for the structure with space group $C2/m$. Hence while $LiNi_{0.5}Mn_{0.5}O_2$ has the same in-plane ordering as Li_2MnO_3, it has a distinctly different ordering along the c axis. If the transition-metal layers were disordered, as speculated previously,[8] both stacking sequences ($C2/m$ and $P3_112$) would be identical and degenerate to the $R\bar{3}m$ structure as a result of the lack of translational symmetry breaking in the transition-metal layer.

It is not possible to determine the occupancies of α and β sublattices directly from the TEM experiments. To generate a model with which to simulate the TEM patterns, 9% Ni occupancy in the lithium layer and a composition of $Li_{0.09}Ni_{0.41}Mn_{0.50}$ with a charge balance of $3+$ in the transition-metal layer were assumed. Small variations in the Ni occupancy value (8-10%) do not affect the conclusions of this article. Given this composition, one cannot create a stoichiometric occupation of α and β sites in the transition-metal layer. However, this does not preclude long-range ordering, which is common even with partial occupancies.[16] Given the charge differ-
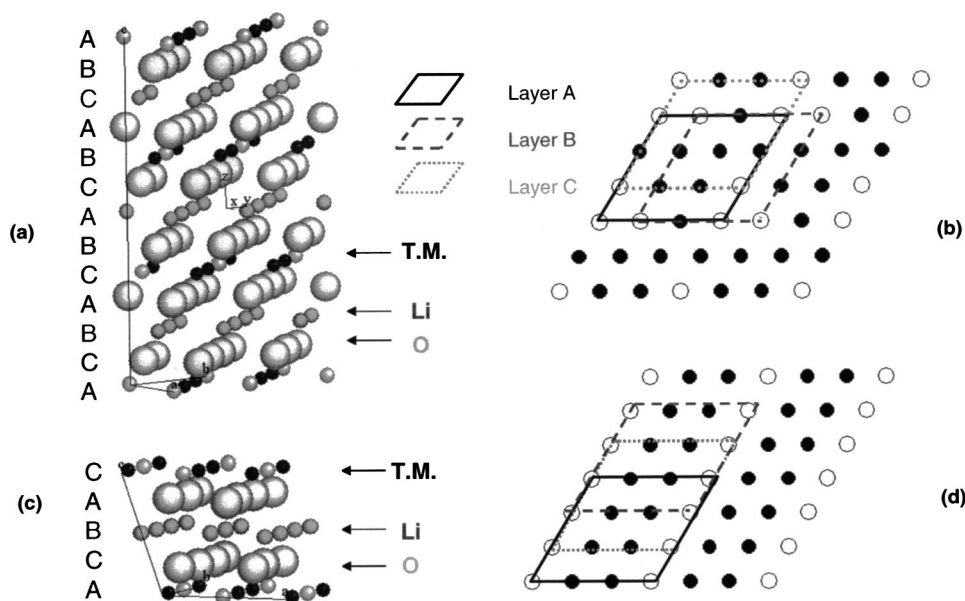
Figure 3. (a) Proposed structure of $LiNi_{0.5}Mn_{0.5}O_2$ with $P3_112$ space group. (b) $[001]_{\text{hex.}}$ projection of transition-metal layers reveals threefold screw axis along the c axis. (c) Structure with the same in-plane ordering, but establishes a different stacking scheme with space group $C2/m$. (d) $[001]_{\text{hex.}}$ projection of transition-metal layers in the structure with space group $C2/m$.
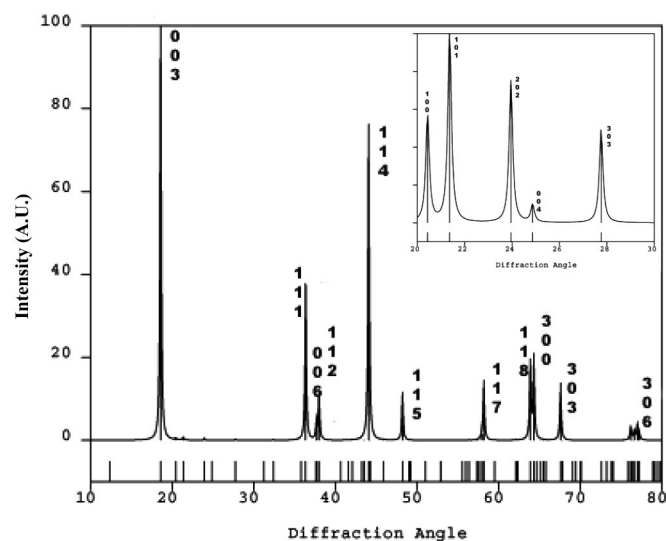
Figure 4. Calculated powder XRD pattern of $LiNi_{0.5}Mn_{0.5}O_2$ with the proposed structure. $\lambda = 1.5406$ Å. Note that the superreflections peak intensities in the range of 20-30° (see inset) are less than 1% of the maximum fundamental reflection peak intensity $(003)_{hex.}$.

ence between Li^+ and Mn^{4+}, one expects a strong ordering tendency between these ions. Experimental XRD evidence for the ordering interaction between Li^+ and Mn^{4+} can be found in the well-ordered nature of Li_2MnO_3, and in the Li NMR observations for this material, which showed a much higher probability for Li^+ ions to be surrounded with 6 Mn^{4+} ions than would be found for a random solution. The maximum number of the nearest neighbor Li^+-Mn^{4+} contacts can be achieved by segregating them to separate sublattices (Li to α, and Mn to β). In addition, first-principle studies have shown that there is a strong tendency for Ni^{2+} and Mn^{4+} to order.[10] The maximum ordering between Ni and Mn occurs when Ni^{2+} preferentially occupies α site. Hence, a likely model for the occupancies in the $\sqrt{3}a_{hex.} \times \sqrt{3}a_{hex.}$ structure with in-plane composition $Li_{0.09}Ni_{0.41}Mn_{0.50}$ is [α (0.27Li; 0.73Ni), β (0.75Mn; 0.25Ni)]. Though less likely, it is conceivable that Li orders with Ni or Mn,

where Ni and Mn ions are randomly interchangeable with each other, which leads to site occupancies [α (0.27Li; 0.33Ni; 0.40Mn), β (0.45Ni; 0.55Mn)].

To understand why ordering in $LiNi_{0.5}Mn_{0.5}O_2$ may have been missed with XRD and neutron diffraction methods, we examine the superlattice peak intensities in simulated powder XRD and neutron diffraction patterns using Cerius.[2] The calculated powder XRD pattern of the $\sqrt{3}a_{hex.} \times \sqrt{3}a_{hex.} \times c_{hex.}$ superstructure with site occupancies α (0.27Li; 0.73Ni) and β (0.75Mn; 0.25Ni) is shown in Fig. 4. Lithium layers in the simulated superstructure consist only of Li, as it can be shown that the random distribution by Ni (8-10%) in the lithium layers has a negligible effect on the superstructure reflection intensity. The superstructure peak intensities are less than 1% of the intensity of the fundamental $(003)_{hex.}$ peak, making them very difficult to resolve experimentally. The low superstructure peak intensities result from similar average scattering factors for X-rays on α (0.27Li; 0.73Ni) and β (0.75Mn; 0.25Ni) sites. Simulated powder XRD diffraction patterns of superstructures with the *abcabc* and *ababab* stacking of the ordered transition-metal layers are nearly identical, which demonstrates the ambiguous nature of structural determination by powder diffraction techniques.

For the site occupancies α (0.27Li; 0.73Ni) and β (0.75Mn; 0.25Ni), one may expect to see relatively strong superstructure peaks in the powder neutron diffraction pattern of the $\sqrt{3}a_{hex.} \times \sqrt{3}a_{hex.} \times c_{hex.}$ superstructure as Ni and Mn have significantly different neutron scattering lengths ($b_{Ni} = 10.30$ fm; $b_{Mn} = -3.73$ fm).[17] However, the neutron scattering length of Li, b_{Li}, is -1.90 fm[17] and Li occupancy on the Ni-rich α site significantly lowers the contrast between α and β in powder neutron diffraction patterns. In the simulated powder neutron diffraction pattern of the superstructure with α (0.27Li; 0.73Ni) and β (0.75Mn; 0.25Ni) in Fig. 5a the superstructure reflection peak intensities are only a few percent of the maximum fundamental reflection peak intensities. Small partial occupancies of Mn on α and Ni on β, further lowers the superreflections peak intensities in powder neutron diffraction. For instance, if 4% Mn and Ni interchange sites, making the occupancy on α [0.27Li; 0.61Ni; 0.12Mn] and β [0.63Mn; 0.37Ni], the intensities of superstructure reflections fall to less than 2% of the maximum fundamental peak intensity, as shown in Fig. 5b. As typical $LiNi_{0.5}Mn_{0.5}O_2$ samples are synthesized at high temperatures, such disorder is likely, making ordering difficult to detect even by neutron diffraction. We therefore believe that the previous conclu-

(a)

(b)
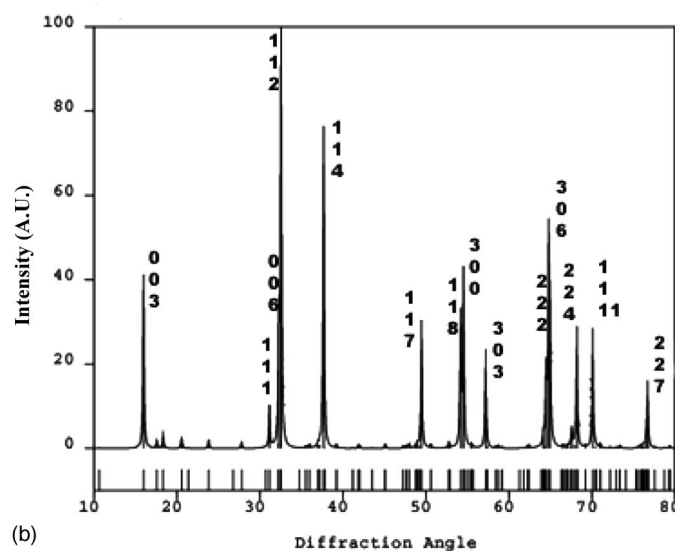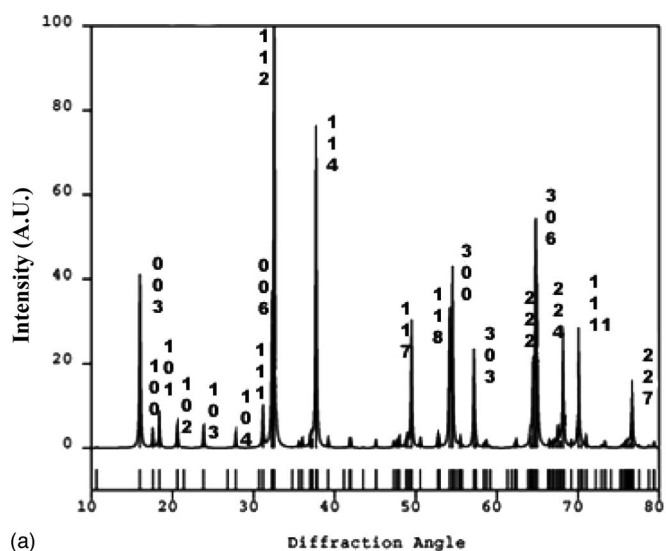
Figure 5. Calculated powder neutron diffraction patterns of proposed superstructures ($\lambda = 1.3260$ Å) with (a) α [0.27Li; 0.73Ni] and β [0.75Mn; 0.25Ni]; (b) α [0.27Li; 0.61Ni; 0.12Mn] and β [0.63Mn; 0.37Ni].

sion that ordering in $LiNi_{0.5}Mn_{0.5}O_2$ is unlikely[8] based on powder XRD and neutron diffraction data should be revisited. We have shown here that even for the maximum long-range ordering of Ni and Mn possible, neutron superstructure peaks appear only with very small intensities.

In this report, we have shown that in $LiNi_{0.5}Mn_{0.5}O_2$ Li, Ni, and Mn are long-range ordered in the transition-metal layer, creating two distinct sites (α and β) in a $\sqrt{3}a_{hex.} \times \sqrt{3}a_{hex.}$ unit cell. We believe that the site with lower (higher) multiplicity is preferentially occupied by Li and Ni (Ni and Mn). Hence, the model we propose has significant ordering between (Li, Ni) and Mn, but without the presence of a distinct Li_2MnO_3 phase, in agreement with our electron diffraction data that show no evidence of secondary phase in the $LiNi_{0.5}Mn_{0.5}O_2$ sample.

In contrast to Li_2MnO_3, the ordered layers are stacked in an *abcabc* sequence along the *c* axis creating a unit cell with $P3_112$ symmetry. The reason for this different stacking between $LiNi_{0.5}Mn_{0.5}O_2$ and Li_2MnO_3 is not clear at this point. Although the ordering may persist over long range, the small X-ray and neutron scattering contrast between α and β sites can make superstructure reflections undetectable, which makes conclusions drawn from XRD and neutron diffraction data alone unreliable.

Since the long-range order parameter depends on synthesis conditions, cooling rate, and stoichiometry control, our result may explain some of the sensitivity on processing conditions found for this material.

Acknowledgment

References

1. T. Ohzuku and Y. Makimura, *Chem. Lett.,* **30**, 744 (2001).
2. Z. H. Lu, D. D. MacNeil, and J. R. Dahn, *Electrochem. Solid-State Lett.,* **4**, A191 (2001).
3. Z. H. Lu, L. Y. Beaulieu, R. A. Donaberger, C. L. Thomas, and J. R. Dahn, *J. Electrochem. Soc.,* **149**, A778 (2002).
4. Y. Makimura and T. Ohzuku, *J. Power Sources,* **119**, 156 (2003).
5. W. S. Yoon, Y. Paik, X. Q. Yang, M. Balasubramanian, J. McBreen, and C. P. Grey, *Electrochem. Solid-State Lett.,* **5**, A263 (2002).
6. J. Reed and G. Ceder, *Electrochem. Solid-State Lett.,* **5**, A145 (2002).
7. Y. Arachi, H. Kobayashi, S. Emura, Y. Nakata, M. Tanaka, and T. Asai, *Chem. Lett.,* **32**, 60 (2003).
8. Z. H. Lu, Z. H. Chen, and J. R. Dahn, *Chem. Mater.,* **15**, 3214 (2003).
9. X. Q. Yang, J. McBreen, W. S. Yoon, and C. P. Grey, *Electrochem. Commun.,* **4**, 649 (2002).
10. W.-S. Yoon, S. Iannopollo, C. P. Grey, D. Carlier, J. Gorman, J. Reed, and G. Ceder, *Electrochem. Solid-State Lett.*, To be published.
11. T. Ohzuku and Y. Makimura, Abstract 1079, The Electrochemical Society Meeting Abstracts, Vol. 2003-1, Paris, France, April 27-May 2, 2003.
12. Y. Shao-Horn, S. Levasseur, F. Weill, and C. Delmas, *J. Electrochem. Soc.,* **150**, A366 (2003).
13. A. Van der Ven, M. K. Aydinol, and G. Ceder, *J. Electrochem. Soc.,* **145**, 2149 (1998).
14. M. E. Arroyo de Dompablo, C. Marianetti, A. Van der Ven, and G. Ceder, *Phys. Rev. B,* **63**, 144107 (2001).
15. P. Strobel and B. Lambertandron, *J. Solid State Chem.,* **75**, 90 (1988).
16. J. M. Cowley, *Diffraction Physics*, North-Holland, New York (1981).
17. National Institute of Standards and Technology Website: http://www.ncnr.nist.gov/resources/n-lengths/